Mon. Not. R. Astron. Soc. **000**, 1–6 (2007) Printed 7 December 2007 (MN LATEX style file v2.2)

On the relativistic iron line and soft excess in the Seyfert 1 galaxy Markarian 335⋆

Paul M. O'Neill,[1,2]† Kirpal Nandra[1]‡, Massimo Cappi[3], Anna Lia Longinotti[4] and Stuart A. Sim[5]

[1]*Astrophysics Group, Imperial College London, Blackett Laboratory, Prince Consort Road, London SW7 2AZ*
[2]*School of Computing & Mathematics, Charles Sturt University, P.O. Box 588, Wagga Wagga NSW 2678, Australia*
[3]*INAF-IASF Bologna, Via Gobetti 101, I-40129 Bologna, Italy*
[4]*XMM-Newton Science Operation Centre, ESAC, ESA, Apartado 50727, E-28080 Madrid, Spain*
[5]*Max-Planck-Institut fur Astrophysik, 85741 Garching, Germany*

Accepted. Received

ABSTRACT

We report on a 133 ks *XMM-Newton* observation of the Seyfert 1 galaxy Markarian 335. The 0.4–12 keV spectrum contains an underlying power law continuum, a soft excess below 2 keV, and a double-peaked iron emission feature in the 6–7 keV range. We investigate the possibility that the double-peaked emission might represent the characteristic signature of the accretion disc. Detailed investigations show that a moderately broad, accretion disc line is most likely present, but that the peaks may be owing to narrower components from more distant material. The peaks at 6.4 and 7 keV can be identified, respectively, with the molecular torus in active galactic nucleus unification schemes, and very highly ionized, optically thin gas filling the torus. The X-ray variability spectra on both long ($\sim$ 100 ks) and short ($\sim$ 1 ks) timescales disfavour the recent suggestion that the soft excess is an artifact of variable, moderately ionized absorption.

Key words: galaxies:individual:Markarian 335 – galaxies:active – galaxies:Seyfert – X-rays:galaxies.

1 INTRODUCTION

Studying the X-ray emission from active galactc nuclei (AGNs) offers the potential of observing relativistic effects. The X-ray emission, being produced deep in the potential well of the putative black hole, is predicted to be affected by gravitational redshift and Doppler effects. Emission lines may thus become broadened and skewed, the line profiles yielding information on the inner accretion flow such as the geometry, disc emissivity and black hole spin (e.g. Fabian et al. 1989; Stella 1990; Laor 1991). The Doppler effects in particular can give rise to a broad Fe Kα line having a characteristic double-horned structure (Chen et al. 1989).

At energies below a few keV, an enhancement of flux above the underlying power law is commmonly seen in AGN spectra. The origin of this so-called 'soft excess' is a long-standing, unsolved puzzle in AGN studies (see review by Mushotzky et al. 1993). The possible identification of the soft excess as owing to inverse-Compton scattering of UV disc photons has been challenged by the apparent rather constant 'temperature' of the excess (e.g., Gierlinski & Done 2004; Crummy et al. 2006). Emission lines associated with disc reflection (e.g. Crummy et al. 2006), or the influence of a moderately ionized 'warm' absorber (Gierlinski & Done 2004), have been proposed recently to explain the soft excess.

The Seyfert 1 galaxy Markarian 335 ($z = 0.0258$) exhibits both a soft excess and a broad emission feature in the region of the iron line. The soft excess has been observed by various missions, starting with *EXOSAT* (Pounds et al. 1987). A *ROSAT* spectrum could be modelled equally well as either a double power-law or a power-law with an absorption edge (Turner et al. 1993). The soft excess in an *ASCA* spectrum could be modelled as either a blackbody (Reynolds 1997), additional steep power law component (George et al. 1998) or reflection from an ionized disc (Ballantyne et al. 2001). Reynolds (1997) found also that the addition of an absorption edge to the underlying hard power-law component improved the fit. A *BeppoSAX* spectrum could be modelled similarly to the *ASCA* spectrum (Bianchi et al. 2001). A narrow iron line, consistent with arising from neutral material, was detected in the *ASCA* spectrum with an equivalent width (EW) of $\sim$ 100 eV (Nandra et al. 1997). When fitted instead with a relativistic line and reflection continuum the EW was $\sim$ 250 eV. The

⋆ Based on observations obtained with XMM-Newton, an ESA science mission with instruments and contributions directly funded by ESA Member States and NASA

† poneill@csu.edu.au
‡ k.nandra@imperial.ac.uk

BeppoSAX spectrum could likewise be modelled with a relativistic line having an EW of a few hundred eV. A narrow line at 6.4 keV is also likely to be present in the *BeppoSAX* data.

XMM-Newton first observed Mrk 335 in 2000 December for 35 ks. Gondoin et al. (2002) found excess emission in the 5–7 keV range above the underlying power-law, which could be described by relativistically blurred emission from highly ionized iron. The combination of reflection from an *unblurred*, highly ionized disc and Bremstrahlung emission was able broadly to describe the entire 0.3–10 keV range, with the reflection flux contributing ~ 50 per cent of the soft excess. Crummy et al. (2006) also analysed these data and were able to model the spectrum as relativistically blurred ionized disc reflection. Importantly, Gondoin et al. (2002) examined the Reflection Grating Spectrometer (RGS) spectrum and found no evidence of absorption or emission from ionized gas. Longinotti et al. (2006) recently reanalysed the European Photon Imaging Camera (EPIC) data from this observation, confirming the existence of a broad emission feature and noting an absorption feature at ~ 5.9 keV.

XMM-Newton re-observed Mrk 335 in 2006 for 133 ks. The purpose of these observations was to better characterise the iron line emission. Moreover, being long and nearly uninterrupted, this observation offers the best data thus far to study the variability. We present here an initial analysis of the data collected by the EPIC PN instrument.

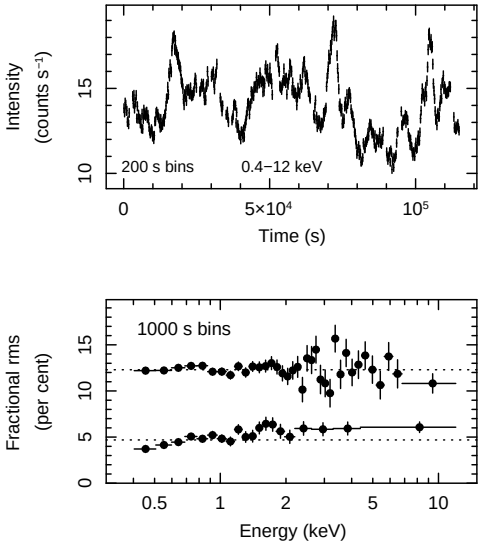

Figure 1. 0.4–12 keV light curve using 200 s bins (top) and fractional rms spectra using 1000 s bins (bottom). The upper spectrum was calculated in the conventional manner, while the lower shows the point-to-point variability. The upper and lower dotted lines show constants of 12.3 and 4.7 per cent, respectively.

2 OBSERVATIONS AND ANALYSIS

XMM-Newton observed[1] Mrk 335 between 2006 January 03 and 05, for a duration of 133 ks. We present here an analysis of the EPIC PN data. The observation was conducted in Small Window mode, thus avoiding photon pile-up, and the Thin filter was used.

Source events were extracted from a circular region, centred at the X-ray centroid, with a radius of 680 detector pixels ($34''$). Background events were extracted from two rectangular regions with a combined area 3.4 times larger than the source region. Background flares were present at the beginning and end of the observation, and the exclusion of these intervals resulted in a low-background duration of 115 ks. The final usable data train contained gaps amounting to ~ 0.3 per cent of this duration.

Source and background light curves were extracted for various energy bands using time resolutions of 200 and 1000 s, and each time bin was required to be fully exposed. The fractional root-mean-square (rms) variability spectrum (see, e.g. Vaughan et al. 2003) was calculated from the 1000 s light curves, each of which comprised 104 bins over the 115 ks duration. The uncertainties in the rms measurements were determined using Monte Carlo simulations. Each simulation involved perturbing the observed counting rates with a Gaussian deviate with a standard deviation equal to the size of the observed error bar. The fractional rms was then calculated from the synthetic light curve. We performed 10,000 such simulations, and the standard deviation of the simulated rms values was adopted as the 1 σ uncertainty owing only to Poisson noise. As well measuring variability in the conventional manner, we also calculated the point-to-point fractional rms spectrum to probes the variability on relatively short timescales (Edelson et al. 2002).

Time-averaged source and background spectra were extracted using the set of events present in the 1000 s light curves. The spectral channels were grouped so that: there were no more that 2 groups per resolution full-width-at-half-maximum, and each group in the source spectrum possessed at least 20 counts. The source region spectrum contained $\sim 1.5 \times 10^6$ counts (0.4–12 keV[2]), of which 0.14 per cent are expected to be background. The quoted uncertainties in the spectral fits correspond to $\Delta\chi^2 = 1$, unless stated otherwise. These may underestimate the true uncertainties when multiple parameters are fitted (Lampton et al. 1976).

3 ENERGY-RESOLVED VARIABILITY

In Fig. 1 (top) we present the 0.4–12 keV light curve, using a time-resolution of 200 s, which has a fractional rms variability of 12.24 ± 0.08 per cent. The rms spectra, calculated using a time resolution of 1000 s, are shown in Fig. 1 (bottom).

The conventional fractional rms spectrum could be satisfactorily described with a constant of 12.3 per cent ($\chi^2/\mathrm{DOF} = 34.6/36$). The point-to-point spectrum, while still being rather flat, cannot be well described with a constant ($\chi^2/\mathrm{DOF} = 72.3/19$). Three energy bands of importance are 0.4–0.8, 0.8–2 and 2–12 keV: an ionized absorber with varying opacity, if present, would induce enhanced variability in the 0.8–2 keV band (Gierlinski & Done 2006). Considering first the conventional rms spectrum, the values in these three bands are 12.35 ± 0.12, 12.32 ± 0.13 and 12.69 ± 0.27 per cent, respectively. The uncertainties in these values suggest that any enhancement in the 0.8–2 keV range is constrained to be less than ~ 0.5 per cent. In the point-to-point rms spectrum the corresponding rms values are 4.23 ± 0.11, 5.20 ± 0.12 and 6.12 ± 0.26 per cent, which reveal the absence of a peak in the 0.8–2 keV range over short timescales.

The fractional rms in the 5.6–7 keV band (i.e., the band containing Fe line emission; see below) is 12.6 ± 0.9 per cent. The time-averaged flux in this band is a factor of 1.12 greater than the

[1] The observation identification number is 0306870101.

[2] 'PI' channels 380–11995.

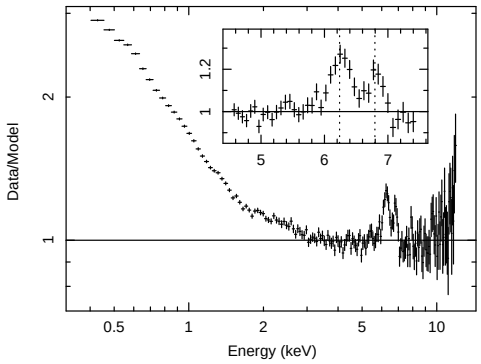

Figure 2. Ratio between the observed flux and the best-fitting power-law fitted over the observed 3–4.5 and 7.5–12 keV energy ranges, showing the iron line and soft excess. The inset shows the double peaked profile. The energy scale corresponds to the observed frame and the left- and right-hand dotted lines indicate rest energies of 6.4 and 6.97 keV, respectively. The highest residual seen at 12 keV contributes only ~ 2 to the χ^2 of the power-law fit.

underlying power-law. If the excess of flux in this band is non-varying, then the rms should be suppressed by the same factor. The uncertainty in the rms is too large to reach a firm conclusion regarding the variability or otherwise of this feature, but it is consistent with being as variable as the power-law.

4 THE TIME-AVERAGED SPECTRUM

4.1 A first look

A power-law modified by Galactic absorption[3] of $N_{\rm H} = 3.99 \times 10^{20}$ cm^{-2} was fitted over the observed frame 3.0–4.5 and 7.5–12 keV energy ranges. The best-fitting power-law had a photon index of $\Gamma = 2.00 \pm 0.01$ with an unabsorbed 2–12 keV flux and luminosity[4] of 1.75×10^{-11} ergs cm^{-2} s^{-1} and 2.66×10^{43} ergs s^{-1}, respectively. The ratio between the observed flux and best-fitting power-law is shown in Fig. 2 (top). The presence of a soft excess is clear, reaching a maximum of ~ 3 times the flux of the extrapolated power-law. Double-peaked line emission is also visible in the 6–7 keV range. Note that the highest residual seen at 12 keV contributes only ~ 2 to the χ^2 of the power-law fit. Unlike the earlier *XMM-Newton* observation (Longinotti et al. 2006) there is no clear absorption feature at ~ 5.9 keV; we leave a detailed investigation for future work.

We initially attempted to parametrize the line complex using models with two or more Gaussians fitted over the 3–12 keV range. A model with two narrow ($\sigma = 1$ eV) lines yielded $\chi^2/{\rm DOF} = 145.4/110$. We allowed the width of the ~ 6.4 keV line to vary, and the fit improved to $\chi^2/{\rm DOF} = 98.4/109$, with rest-frame line energies of 6.42 ± 0.02 keV (broad line) and 7.00 ± 0.02 keV (narrow line). These energies are consistent with those expected for Fe I Kα and Fe XXVI Lyα, respectively. The width of the broad line was $\sigma = 0.19 \pm 0.03$ keV, and the EWs of the broad and narrow lines, respectively, were 127 ± 17 and 42 ± 7 eV. We then added a narrow line and the fit improved to $\chi^2/{\rm DOF} = 95.0/107$. The two narrow lines had best-fitting energies of 6.40 ± 0.04 and 7.00 ± 0.03 keV, and the corresponding EWs were, respectively, 20 ± 9 and 36 ± 8 eV. The broad line had a best-fitting energy, width and EW of 6.43 ± 0.05, 0.27 ± 0.06 keV and 115 ± 14 eV, respectively. The joint confidence intervals of the 6.4 keV line fluxes indicate that these are greater than zero with a significance of 91 (narrow line) and > 99.99 per cent (broad line). We then replaced the broad Gaussian with two narrow lines and the fit worsened to $\chi^2/{\rm DOF} = 103.5/106$, with line energies of 6.28 ± 0.02 and 6.65 ± 0.04 keV.

A double-peaked profile is a natural characteristic of relativistic disc lines, so it may be possible to interpret the entire line profile in this framework, with the 6.4 keV peak representing the red horn and the 7 keV peak the blue horn. We test this explicitly below.

4.2 Neutral disc iron line

To model reflection from a neutral disc we have modified the reflection continuum model PEXRAV (Magdziarz & Zdziarski 1995). The enhanced model, which we refer to as PEXMON, includes the Fe Kα (including the Compton shoulder), Fe Kβ and Ni Kα emission lines (see Nandra et al. 2007, for more details). The dependence of line flux on photon-index and inclination is based on the results of George & Fabian (1991). In PEXMON the reflection continuum and emission line fluxes are linked, as expected from physical models, and the constraints on the 'reflection fraction' are largely from the Fe Kα line. To construct a disc line model we convolved a PEXMON component with the relativistic blurring model KDBLUR2, which itself uses the kernel of the LAOR disc line model (Laor 1991; Fabian et al. 2002). Following Nandra et al. (2007), the disc emissivity power-law index was fixed to break from a value of 0 within the 'break radius', $r_{\rm br}$, to a value of -3 for larger radii. The disc inner radius was fixed at its minimum value of 1.235 $r_{\rm g}$, which corresponds to the innermost stable orbit for a maximally spinning black hole, and the outer radius was fixed at the maximum permitted model value of 400 $r_{\rm g}$. The inclination and $r_{\rm br}$ were free to vary. With the assumed emissivity, this model well approximates a point source illuminating a slab, with a peak emissivity at $r_{\rm br}$ and a height of the same order. Note that this emissivity law is non-relativistic, and does not account for enhanced inner disc reflection owing to light bending effects (e.g. Martocchia et al. 2000).

A single neutral disc line was unable to model the entire line profile. A large component of line flux is required at the Fe I rest energy of 6.4 keV. This would require the red-horn to be only slightly shifted in energy via gravitational and Doppler effects. It is not possible to then also produce a blue horn that is significantly shifted from 6.4 keV. Moreover, the blue horn is expected to be more intense than the red horn.

We therefore attempted to model the profile with a combination of distant, neutral reflection and a disc line. The former component is intended to account primarily for the narrow emission at 6.4 keV and we modelled it using an unblurred PEXMON component with a fixed inclination of 60 degrees. The disc line, on the other hand, is intended to model the blue wing and broad component of the profile. This model yielded a satisfactory fit ($\chi^2/{\rm DOF} = 99.0/110$). The break radius was constrained to be less than 70 $r_{\rm g}$ (95 per confidence), with a best-fitting value of 4 $r_{\rm g}$. While the overall shape of the profile is reproduced, the blue-horn in this model is unable to account for the sharpness of the observed line at 7 keV.

We next explored the possibility that there is an Fe XXVI Lyα emission component contributing to the blue wing. This line might physically be produced via fluorescence in optically thin plasma.

[3] The Galactic NH was obtained using the NASA HEASARC 'nH' tool, http://heasarc.gsfc.nasa.gov/docs/tools.html .

[4] The values $H_0 = 70$ and $\lambda_0 = 0.73$ were used in calculating the luminosity.

We added a narrow ($\sigma = 1$ eV) Gaussian with a fixed energy of 6.97 keV to the best-fitting disc line model. The fit was significantly improved ($\chi^2/\mathrm{DOF} = 89.2/109$), with a reduction in χ^2 of 9.8. The break radius and inclination were poorly constrained, with the one-sided 95 per cent confidence intervals ($\Delta\chi^2 = 4.61$) restricting the radius and inclination, respectively, to $> 15\,\mathrm{r_g}$ and > 22 degrees. Indeed, varying r_{br} through values above about $\sim$150 $\mathrm{r_g}$ did not yield any variation in χ^2. Relative to the power-law continuum, the reflection fraction of the blurred PEXMON component was 0.6 ± 0.1, which corresponds to the disc subtending a solid angle of 1.2π for a slab geometry. The reflection fraction of the unblurred PEXMON component and the EW of the Fe XXVI Lyα line were 0.31 ± 0.08 and 34 ± 7 eV, respectively, and the line flux was $(4.7 \pm 1.0) \times 10^{-6}$ photons cm^{-2} s^{-1}.

Finally, we removed the PEXMON component representing distant reflection to investigate whether the profile could be modelled with only a relativistic disc line and a narrow Fe XXVI Lyα line. In this case the best-fitting break radius was constrained to be above $\sim$100 $\mathrm{r_g}$, and the reflection fraction increased to 0.7 ± 0.1. The fit became significantly worse, with χ^2 increasing by 7.4.

4.3 Ionized disc iron line

Part of the difficulty in reproducing the observed profile with a neutral disc line is that, in order to reproduce the sharp blue peak at ~ 7 keV, a relatively high inclination with minimal gravitational broadening is required. However, the *red horn* in such a model, being narrow and at an energy below 6.4 keV, fails to fit the broad observed excess around the Fe I rest energy. An ionized disc, on the other hand, can produce Fe lines with rest energies between 6.4 and 7 keV. With variable ξ and inclination an ionized disc model might, then, be flexible enough to describe the observed profile.

To construct an ionized disc line model we used the REFLION[5] model (Ross & Fabian 2005), which incorporates both line emission with Compton broadening and the reflection continuum. REFLION is defined at a limited number of values of ionization parameter, ξ, and Γ, and interpolation between these grid points may yield deviations from the true model spectrum (2006, R. Ross, priv. comm.). We consider ξ to be a free parameter but keep its value fixed during minimisation.

We constructed a model comprising distant reflection (PEXMON), plus relativistically blurred ionized reflection (KDBLUR2 and REFLION), plus a narrow Fe XXVI Lyα line. The ionization parameter was fixed at the minimum permitted value of $\xi = 30$, which yielded $\chi^2/\mathrm{DOF} = 87.4/108$. We then increased ξ to its next defined value of $\xi = 100$, and the best-fitting model yielded $\chi^2 = 87.8/108$. When the ionization was increased further, to $\xi = 300$, the fit worsened to $\chi^2 = 99.2/108$. An ionized disc model is thus not preferred over a neutral disc. We repeated these three fits without a narrow line at 6.97 keV, and confirmed that, as for the neutral disc model, the inclusion of the Fe XXVI Lyα line improved the fit.

4.4 Partial covering absorber

The broad emission feature in the earlier *XMM-Newton* spectrum could be well-described by either a relativistic disc line (the preferred interpretation) or a neutral partial covering absorber model (Longinotti et al. 2006). One of the goals of obtaining the recent, longer observation was to break the degeneracy between these two interpretations. We have, therefore, attempted to fit the new data with a partial covering model.

We initially fitted the spectrum with a partial covering absorber plus a PEXMON component to represent distant, neutral reflection, which yielded $\chi^2/\mathrm{DOF} = 101.9/111$. The addition of a narrow Fe XXVI Lyα emission line improved the fit ($\chi^2/\mathrm{DOF} = 96.0/110$), with a covering fraction of 36 ± 6 per cent. This model, while yielding a worse fit compared to the neutral disc line, is formally acceptable, so we cannot rule out a partial covering interpretation. The best-fitting photon index for this model is $\Gamma \sim 2.3$, compared to $\Gamma \sim 2.1$ for the neutral disc line model.

4.5 The soft excess

The REFLION model includes the soft X-ray line emission that is proposed by, e.g., Crummy et al. (2006) to explain the soft excess. Detailed modelling of the soft excess is beyond the scope of this Letter. However, to determine roughly the extent to which the soft excess might be attributed to ionized reflection we examined the ratio between the observed spectrum in the 0.4–3 keV range and the extrapolated best-fitting 3–10 keV ionized disc model.

We initially used the best-fitting model with $\xi = 30$ and Solar Fe abundance. The observed flux at 0.4 keV is ~ 2.2 times greater than the extrapolated model. Crummy et al. (2006) fitted the earlier *XMM-Newton* observation with an Fe abundance of 0.7. We therefore reduced the abundance to 0.5, which is the closest value to 0.7 for which REFLION is defined. This reduces the Fe line flux relative to the soft flux. We refitted the 3–10 keV spectrum and the 0.4–3 keV residuals were up to a factor of ~ 1.6 above the extrapolated model. Reducing the abundance to the next lowest defined value of 0.2 yielded a significantly worse 3–12 keV fit ($\Delta\chi^2 = 19.5$).

We then increased the ionization parameter to $\xi = 300$, with an Fe abundance of 0.5. This increased the model soft flux and reduced the 0.2–3 keV residuals to be up to a factor of only ~ 1.1 above the model. However, the rather smooth shape of the soft excess below 2 keV is not reproduced. An increase in the relativistic blurring could produce a smoother spectrum, but in our simple test the disc line parameters are constrained by the requirement to fit the 3–12 keV spectrum.

5 DISCUSSION

We have conducted an initial analysis of a 133 ks *XMM-Newton* observation of the Seyfert 1 galaxy Markarian 335. The time-averaged spectrum in the 3–12 keV range could be described as a power law continuum ($\Gamma = 2.00 \pm 0.01$) with a double peaked emission feature in the 6–7 keV range. A strong soft excess is present below ~ 3 keV.

5.1 The Fe Kα emission

A relativistic disc line alone could not describe the line profile. A model comprising a disc line and reflection from neutral, distant material yielded a satisfactory fit. The blue horn in the best-fitting disc line is not able to describe very well the sharpness of the observed peak. Increasing the disc ionization did not improve the fit. However, the addition of Fe XXVI Lyα emission did significantly improve the fit. The iron line profile is, then, likely owing to a superposition of distant reflection from neutral material, relativistically blurred reflection from a neutral accretion disc and a narrow

[5] http://heasarc.gsfc.nasa.gov/xanadu/xspec/models/reflion.html

emission line from highly ionized gas. Note that the level of relativistic blurring in our fit is rather moderate. Therefore, our physically motivated emissivity law (see Section 4.2) is preferred over the often-used *unbroken* powerlaw.

We identify the distant reflection component as originating from the torus in AGN unification schemes. For the torus geometry defined in Ghisellini et al. (1994), an assumed PEXMON inclination angle of 60 degrees corresponds to a torus half-opening angle of $\sim$30 degrees. The observed PEXMON component has a reflection fraction of 0.31 ± 0.08, compared to a value of $\sim$0.9 expected for the assumed opening angle. This discrepancy is perhaps explained by the opening angle being greater than assumed. A half opening angle of ~ 75 degrees yields a reflection fraction compatible with that observed. The reflection flux depends on the optical depth on the torus (Ghisellini et al. 1994), and this might also explain the low observed reflection fraction. The reflection fraction of both the distant and the disc line components are well within the ranges observed in other Seyfert galaxies (e.g. Nandra et al. 2007).

The Fe XXVI Lyα emission line, being narrow, must originate from optically thin material. An ionized disc, for example, cannot produce such a narrow line, owing to Compton broadening. The thin gas might be identified as the hot gas that fills the torus and which is responsible for scattering the broad line optical emission into the line of sight (Krolik & Kallman 1987; Antonucci & Miller 1985). An Fe XXVI absorption edge at 9.29 keV should accompany the Fe XXVI Lyα line. For a fluorescent yield of 0.7, the upper limit on the Fe XXVI absorption edge flux in the spectrum, together with the observed line flux, corresponds to a 95 per cent *lower* limit on the covering fraction of $\sim$100 per cent. This rather large fraction can perhaps be explained if the torus does not obscure the hot gas on the far side of the nucleus, and there may be a deficit of gas in the line-of-sight to the central engine.

A partial covering interpretation for the line profile was satisfactory, yet worse than disc reflection. Partial covering yields a steeper photon index than for the disc line, so high energy data (e.g., *Suzaku*) will be able to robustly distinguish between these two interpretations (see, e.g. Reynolds et al. 2004).

5.2 The soft excess

The soft excess seen in many AGN X-ray spectra is possibly an artifact of ionized absorption. The RGS data from the previous *XMM-Newton* observation of Mrk 335 (Gondoin et al. 2002), however, revealed no evidence for absorption or emission from ionized gas. We visually inspected the combined fluxed RGS spectrum from the new data and the only clear feature is an O I absorption line at 0.54 keV. However, this lack of lines is possibly owing to strong Doppler smearing (Gierlinski & Done 2004).

A moderately ionized absorber can yield a soft excess of the kind observed in Mrk 335, where absorption by OVII, OVIII and Fe-L are important. For lower ξ the soft spectrum would show heavy absorption, whereas for very high ionization no significant effects on the soft spectrum would be seen at all. For the absorbers proposed to explain soft excesses, Gierlinski & Done (2006) argued that variations in the continuum luminosity will necessarily induce variations in ionization, and they predicted excess variability around 1 keV. Therefore, the presence of an absorber might be inferred by enhanced variability in the 0.8–2 keV range. Mrk 335 exhibits no such enhancement, so we cannot invoke a moderately ionized absorber with varying ξ to explain its soft excess. It is worth noting that a flat rms spectrum might be produced either in the presence of *non-varying* absorption or in the context of a partial covering absorber model (see Boller et al. 2002; Tanaka et al. 2004, for the case of 1H 0707$-$495).

Perhaps, then, the excess is owing to disc reflection. Crummy et al. (2006) used an iron abundance of 0.7 were able to satisfactorily fit the earlier *XMM-Newton* observation of Mrk 335. The purpose of our simple test was to investigate the extent to which the disc line model could explain the soft excess. When we extrapolated the best-fitting 3–12 keV model down to soft energies we found that disc reflection underpredicts the soft excess flux by up to a factor of $\sim$ 1.6, even with a reduced Fe abundance of 0.5. Increasing the disc ionization reduced the residuals, but the observed soft excess continuum is much smoother than the model. A more complicated reflection model could perhaps be invoked. For example, the soft flux might originate from very close to the black hole, in a region that is both ionized and highly smeared, while the Fe line flux is owing to neutral reflection from further out in the disc. We note in passing that a flat rms spectrum might be associated with 'regime I' in the so-called 'light bending model' (Miniutti & Fabian 2004). However, the relatively large source height inferred from our disc line modelling, and the low reflection flux, is inconsistent with this regime.

ACKNOWLEDGMENTS

The authors acknowledge financial support from PPARC (PMO) and the Leverhulme trust (KN). We thank Andy Fabian for the relativistic blurring code and Randy Ross for assistance with REFLION.

REFERENCES

Antonucci R. R. J., Miller J. S., 1985, ApJ, 297, 621
Ballantyne D. R., Iwasawa K., Fabian A. C., 2001, MNRAS, 323, 506
Bianchi S., Matt G., Haardt F., Maraschi L., Nicastro F., Perola G. C., Petrucci P. O., Piro L., 2001, A&A, 376, 77
Boller Th., et al., 2002, MNRAS, 329, L1
Chen K., Halpern J. P., Filippenko A. V., 1989, ApJ, 339, 742
Crummy J., Fabian A. C., Gallo L., Ross R. R., 2006, MNRAS, 365, 1067
Done C., Madejski G. M., Mushotzky R. F., Turner T. J., Koyama K., Kunieda H., 1992, ApJ, 400, 138
Edelson R., Turner T. J., Pounds K., Vaughan S., Markowitz A., Marshall H., Dobbie P., Warwick R., 2002, ApJ, 568, 610
Fabian A. C., Rees M. J., Stella L., White N. E., 1989, MNRAS, 238, 729
Fabian A. C., et al., 2002, MNRAS, 335, L1
George I. M., Fabian A. C., 1991, MNRAS, 349, 352
George I. M., Turner T. J., Netzer H., Nandra K., Mushotzky R. F., Yaqoob T., 1998, ApJS, 114, 73
Ghisellini G., Haardt F., Matt G., 1994, MNRAS, 267, 743
Gierlinski M., Done C., 2004, MNRAS, 349, L7
—, 2006, MNRAS, 371, L16
Gondoin P., Orr A., Lumb D., Santos-Lleo M., 2002, A&A, 388, 74
Krolik J. H., Kallman T. R., 1987, ApJ, 320, L5
Lampton M., Margon B., Bowyer S., 1976, ApJ, 208, 177
Laor A., 1991, ApJ, 376, 90
Longinotti A. L., Nandra K., Petrucci P. O., O'Neill P. M., 2004, MNRAS, 355, 929

Longinotti A. L., Sim S. A., Nandra K., Cappi M., 2006, MNRAS, in press
Magdziarz P., Zdziarski A., 1995, MNRAS, 273, 837
Martocchia A., Karas V., Matt G., 2000, MNRAS, 312, 817
Miniutti G., Fabian A. C., 2004, MNRAS, 349, 1435
Mushotzky R. F., Done C., Pounds K. A., 1993, ARA&A, 31, 717
Nandra K., George I. M., Mushotzky R. F., Turner T. J., Yaqoob T., 1997, ApJ, 476, 70
Nandra K., O'Neill P. M., George I. M., Reeves J. N., Turner T. J., 2007, MNRAS, in preparation
Pounds K. A., Stanger V. J., Turner T. J., King A. R., Czerny B., 1987, MNRAS, 224, 443
Reynolds C. S., 1997, MNRAS, 286, 513
Reynolds C. S., Wilms J., Begelman M. C., Staubert R., Kendziorra E., 2004, MNRAS, 349, 1153
Ross R. R., Fabian A. C., 2005, MNRAS, 358, 211
Stella L., 1990, Nat, 344, 747
Tanaka Y., Boller Th., Gallo L., Keil R., Ueda Y., 2004, PASJ, 56, L9
Turner T. J., George I. M., Mushotzky R. F., 1993, ApJ, 412, 72
Vaughan S., Edelson R., Warwick R. S., Uttley P., 2003, MNRAS, 345, 1271